Numerical Study of Nanoscaled Granular Giant Magnetoresistance Sensors for the Limit Case of Dipolar Coupled Nanoparticles

A. Weddemann[1], J. Meyer[*2], A. Hütten[2]

[1]Laboratory for Electromagnetic and Electronic Systems, Massachusetts Institute of Technology, 77 Mass Ave, Cambridge, MA 02139, USA

[2]Department of Physics, Thin Films and Physics of Nanostructures, Bielefeld University, PB 100131, 33501 Bielefeld, Germany

[*]jmeyer@physik.uni-bielefeld.de

***Abstract*-Assemblies of highly ordered magnetic nanoparticles dominated by dipolar particle coupling are analyzed in respect to their capability to act as a magnetic field sensor. We demonstrate a wide range of possibilities to tailor the response properties of the sensor to specific demands by either modification of the nanocomponents or the structure as a whole. Additionally, we find that increased detection sensitivity may be bought at the cost of an inherent noise signal. This behavior is contributed to the existence of four distinct operation modes each governed by a different energy contribution within the assembly.**

Keywords- ***Granular Giant Magnetoresistance; Dipolar Coupling; Assembly of Magnetic Nanoparticles; Detection Sensitivity***

I. INTRODUCTION

An important type of magnetic field sensor is based on magnetoresistive effects. A simple setup is shown in Fig. 1(a), two ferromagnetic layers are separated by a non-magnetic, insulating or conducting [1, 2] spacer barrier. The electric resistance of the device depends on the relative orientation of the magnetizations in the two layers and is low for a parallel and high for an antiparallel configuration due to an increased scattering probability of the conducting electrons in the latter case. These devices have found a wide range of applications, e.g., in the field of lab-on-a-chip technologies, where small magnetic particles can be monitored due to the interaction between their magnetic stray fields and the magnetization distribution within the sensing layer [3-5].

Recent trends in edge cutting technological methods venture into a progressive miniaturization of functional devices down to the micro- or even nanoscale [6]. On these scales, the dynamics of such a device are increasingly dominated by magnetic exchange coupling which results in a low degree of curvature in the components of the magnetic distribution. Such type of magnetic stiffness entails finite size effects, which form the reason why magnetic nanoparticles can usually be assumed to be homogeneously magnetized [7]. On the respective length scale, stable magnetic equilibrium states are separated by high energy barriers, e.g., introduced by a uniaxial magnetocrystalline anisotropy [8, 9] which significantly decreases the device sensitivity and the measurable response to an external perturbation may fall below the thermal noise ratio.

A possibility to overcome these finite size effects is the introduction of magnetic domains via spatial separation of the magnetic material itself. As originally shown by Berkowitz et al. [10] and, independently, by Xiao et al. [11], magnetic nanoparticles encapsulated in a metallic matrix show a granular giant magnetoresistance (GMR) effect. The scattering probability of the conducting electrons is high if a low degree of magnetic order can be found along the assembly and low in the opposite case as schematically shown in Fig. 1(b).

II. NUMERICAL MODEL

In order to predict the response of an assembly of magnetic nanoparticles to an external perturbation, the magnetic equilibrium state of the configuration needs to be calculated. Therefore, the Landau-Lifshitz equation [12] for an ensemble of N particles is solved. Due to the above mentioned finite size effects, these particles are homogeneously magnetized and may be approximated by magnetic dipoles. In the following we will restrict our analysis to the limit case of pure dipolar coupling, in order to obtain a first idea of the behavior of this type of sensor devices.

DOI: 10.5963/JBAP0202004

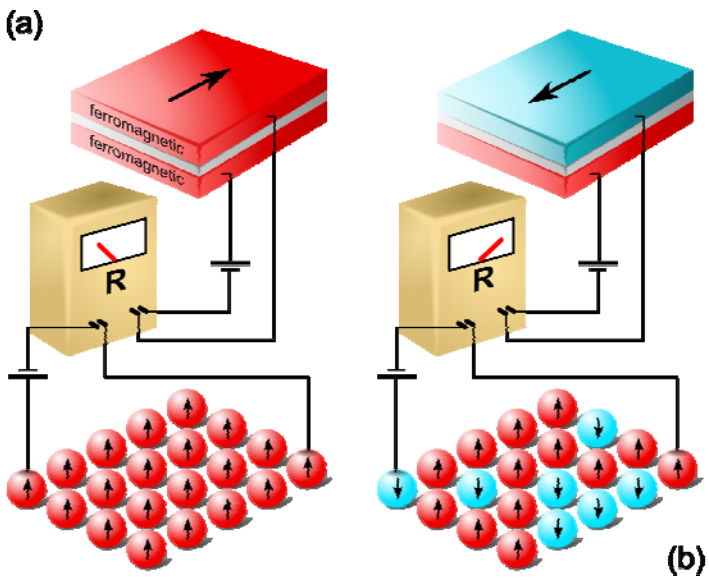

Fig. 1 Schematic representation of two-dimensional magnetoresistive devices
(a) Continuous ferromagnetic multilayer systems and (b) granular layers of magnetic nanoparticles
The electric resistance is low for parallel and high for antiparallel magnetic configurations

The dynamic equations for N interacting particles may be written in matrix form [13]

$$(Id - \alpha \mathrm{M})\frac{\partial \hat{\boldsymbol{m}}}{\partial t} = \gamma \mathrm{M}\, \boldsymbol{H}_{\mathrm{eff}}, \qquad (1)$$

$$|\hat{\boldsymbol{m}}| = 1$$

where γ denotes the gyromagnetic ratio and α the phenomenological damping constant. Further, the following definitions were employed

$$\mathrm{M} = \begin{pmatrix} \mathrm{M}_1 & & 0 \\ & \ddots & \\ 0 & & \mathrm{M}_N \end{pmatrix}$$

with $\mathrm{M}_n = \varepsilon_{ijk}\hat{m}_{n,j}$, $n = 1, \ldots, N$, and the vectors

$$\frac{\partial \hat{\boldsymbol{m}}}{\partial t} = \frac{\partial}{\partial t}(\hat{m}_{x,1}, \hat{m}_{y,1}, \hat{m}_{z,1}, \hat{m}_{x,2}, \ldots)^T$$

$$\boldsymbol{H}_{\mathrm{eff}} = (H_{\mathrm{eff},x,1}, H_{\mathrm{eff},y,1}, H_{\mathrm{eff},z,1}, H_{\mathrm{eff},x,2}, \ldots)^T.$$

The effective magnetic field $\boldsymbol{H}_{\mathrm{eff}}$ may be decomposed according to

$$\boldsymbol{H}_{\mathrm{eff}} = -\frac{\delta f_{ani}}{\delta \boldsymbol{m}} + \boldsymbol{H}_{\mathrm{ext}}. \qquad (2)$$

The strong exchange coupling effects on the considered size scales are taken into account by the assumption that particles do not have a magnetic substructure, but are homogeneously magnetized. f_{ani} describes the anisotropy energy functional and $\boldsymbol{H}_{\mathrm{ext}}$ external magnetic field contributions, which are given by the sum of the dipolar stray field contributions of contiguous particles. Due to the rapidly decreasing field strength ~ $1/r^3$, we apply a cut-off value of $R_S = 5 \times \langle R \rangle$ according to [14] with $\langle R \rangle$ the average particle radius. The equilibrium state of Equation (1) was solved by time integration by a backward differentiation formula of order 4.

III. GENERAL PROPERTIES

Typical solutions of ensembles, which consist of 64 particles positioned along a cubic grid, are presented in Fig. 2.

DOI: 10.5963/JBAP0202004

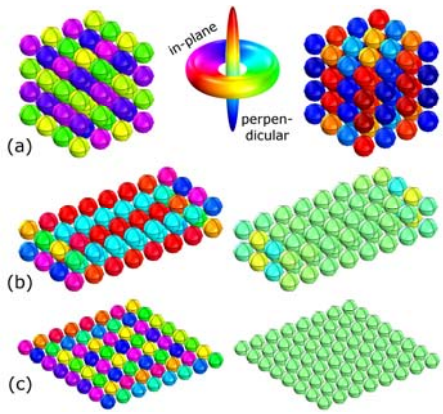

Fig. 2 Magnetic equilibrium states of 64 nanoparticles, which interact via dipolar coupling
The left side shows the in-plane magnetization distributions (color code: disc), the right side the out-of-plane contributions (color code: cone).
In all different spatial configurations, the global and local magnetization of the assembly goes to zero.
Such local effect is a direct consequence of the absence of exchange coupling. For increasing aspect ratio, (a) → (c),
the magnetic orientation is dominated by the geometric structure and no out-of-plane contributions can be found

The left-side plots show the azimuthal component of the normalized magnetization vector $\hat{\boldsymbol{m}}$ (color code: disc), the right side the respective out-of-plane contribution (colour code: cone). The minimization of stray field energy is the driving force of the system. Consequently, due to the absence of exchange coupling between individual colloids, magnetic moments reach orientations that result in a globally and locally vanishing sample magnetization, which is different for the strongly coupled continuous layers. Further, a high aspect ratio results in a strong in-plane confinement of the magnetic moment vectors. This observation is similar to the situation of continuous sensors as long as no strong perpendicular anisotropy is at hand. Therefore, such granular systems maintain the two-dimensional magnetic distributions of continuous films, while they also have an additional magnetic substructure due to the absence of exchange coupling.

Via the introduction of a magnetic substructure into two-dimensional thin film systems, we obtained a promising candidate for a magnetoresistive field sensor on the nanoscale. In order to analyze the properties of these structures, the electric transport characteristics in response to an external magnetic field were calculated.

The granular GMR-effect may be evaluated according to [15]

$$\mathrm{GMR} = 1 - \frac{C}{2}\langle 1 + \cos\theta \rangle^2 \tag{3}$$

where the constant C is a measure for the spin dependence of electron scattering and θ the angle between adjacent magnetic moments. For the sake of simplicity, we will set $C = 1$ in the following. Responses of these assemblies to an external magnetic field are shown in Fig. 3.

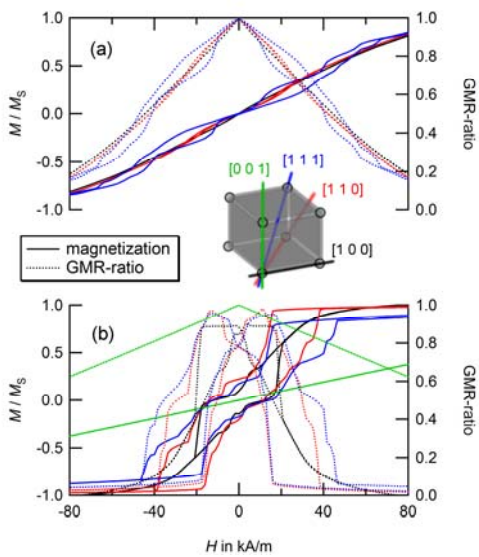

Fig. 3 Response properties of the assemblies shown in Fig. 2 to an external magnetic field for (a) the configuration 4 × 4 × 4 and (b) 8 × 8 × 1
Calculations are carried out for indicated field directions. Due to the symmetry of the particle assembly, the [0 0 1]-direction is equivalent to a measurement to the [1 0 0]-axis for the cubic array (a) and, therefore, not shown in the plot. The cubic array shows an almost isotropic response while particle sheets behave highly anisotropic. In particular, the out-of-plane calculations show paramagnetic behavior (green line)

DOI: 10.5963/JBAP0202004

While the cubic assembly 4 × 4 × 4 exhibits an almost hysteresis free, isotropic, paramagnetic behavior, the planar configuration entails an anisotropic response. We find a hysteretic characteristic for an in-plane contribution and a perfectly paramagnetic behavior of low susceptibility in comparison to the cubic case for out-of-plane contributions (green line). For future experimental realizations, this may already be seen as an indication, that many of the properties of monolayers are lost once smaller clusters can be found in the sample. The resulting structures allow for out-of-plane magnetic components, which alter the GMR-response.

In regard to common preparation procedures, hexagonal assemblies may be realized much easier than cubic structures. As shown in Fig. 4, the geometric microstructure effects the magnetic configuration.

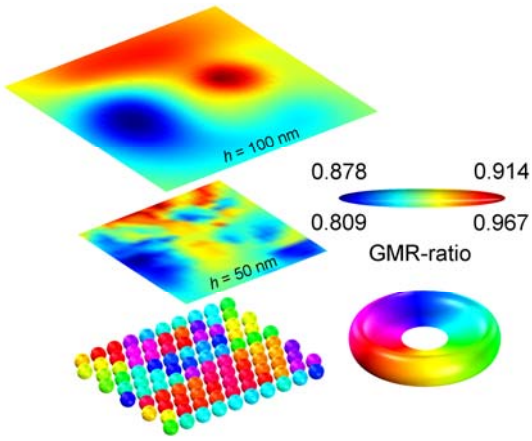

Fig. 4 Equilibrium state of 10 × 10 magnetic nanoparticles assembled in a hexagonal symmetry (bottom)
The plain maps show the response of the assembly to a probe particle placed within the respective plane for two different heights *h*.
An increased GMR-amplitude is bought at the cost of an inherent noise signal, if the distance of the magnetic source is decreased

The local magnetization still vanishes, but loop-like structures as seen in the cubic lattices can no longer be found. As a reference system, an array of 10 × 10 particles of radius R = 8 nm assembled in a hexagonal symmetry of lattice constant a = 20 nm, of a magnetization of MS = 1000 kA/m and without magnetic anisotropy is chosen in the following. The response properties of such an array may be manipulated via the choice of different species of nanocomponents, Fig. 5. In particular, this allows for the adjustment of a device to a specific functional task or measurement type.

Such calculations already show, that these granular films may act as a magnetic field sensor as long as the area of operation is chosen along one of the response slopes, where there is a biunique relation between GMR-response and applied field. A different application field of increased complexity is the spatial detection and magneto optical observation of small magnetic sources such as a particle which travels in a fluid flow or is attached as a marker to a larger biomolecule. In order to analyze the capability of the sensor to determine the position of such a point source, a probe particle magnetized along the z-axis of radius R = 10 nm and magnetization MP = 1000 kA/m was placed along the nodes of grid above the sensor. The dipolar magnetic stray field influences the magnetic configuration of the particle sheet. Thus, the presence of an external perturbation source entails a change of the electric resistance. The strength of this effect depends on various aspects such as the local magnetic orientation within different nanoparticles and is, therefore, depending on the position of the probe particle. Response maps are shown in the top part of Fig. 4, the color code indicates minimum (blue) and maximum (red) response areas, absolute values are given on the right side.

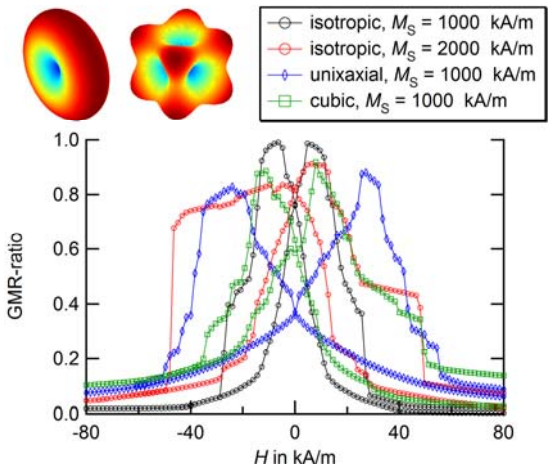

Fig. 5 Response properties of 10 × 10 particles assembled in a hexagonal symmetry with a lattice constant of 20 nm, a radius of *R* = 8 nm and different assumptions for the magnetic properties

DOI: 10.5963/JBAP0202004

If the probe particle is placed at a height of h = 100 nm, a smooth response characteristic is obtained which resembles the response signal of continuous sensors and may be employed in a similar way to obtain an estimation of the particle position [16]. We will not go into details here because the GMR-amplitude ΔGMR is very low. A strong increase of this value of about a factor of 4 can be reported, if the height is decreased to h = 50 nm. However, the response is no longer smooth, the increased effect is bought at a cost. Since no thermal effects are included in our model, the noise is inherent to the device itself.

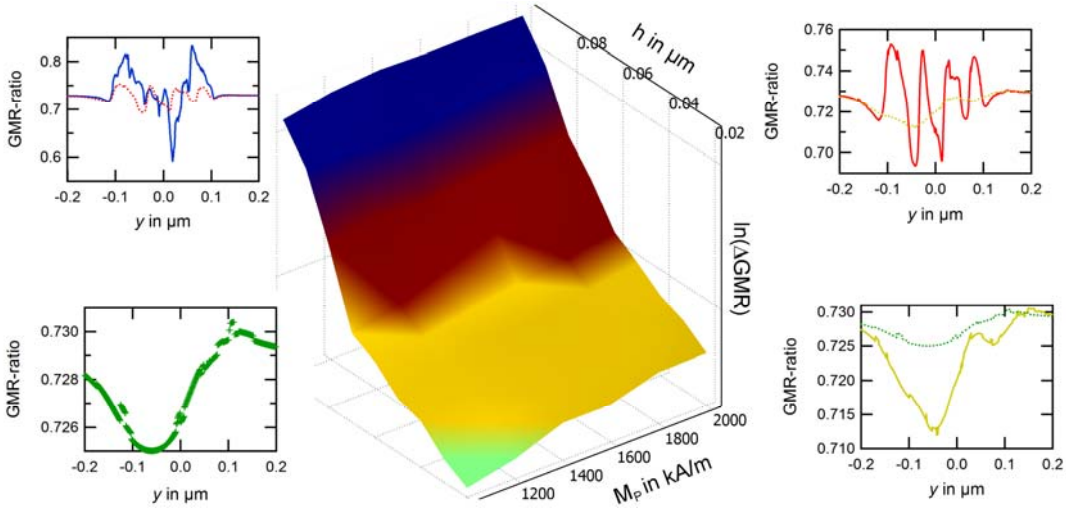

Fig. 6 Response amplitudes in dependency of the probe particle magnetization and its height above the sensor
As indicated by colour, four different response regimes can be identified: linear answer (green), boundary answer (yellow), domain answer (red) and direct answer (blue) regimes

IV. GRANULAR GMR-SENSORS

In order to analyze the origin of the appearance of this type of inherent noise, the response characteristic for a probe particle moved along the line $x = 0$ from $y = -200$ to 200 nm in 101 equidistant steps for different probe particle heights and magnetizations is calculated. The magnetic orientation of the source dipole with $R = 10$ nm is chosen parallel to the out-of-plane direction. The nanocomponents of the particle assembly are set to isotropic 8 nm colloids of $M_S = 500$ kA/m.

All calculations were carried out by the employment of a defined equilibrium state as initial condition, in order to prevent hysteretic effects. The resulting values of the logarithmic GMR-amplitude ΔGMR are shown in Fig. 6 (center), numeric values can be found in Table 1. The color code in the figure indicates distinct response behaviors if the particle is placed at different positions along the line. Typical examples are shown in the insets of Fig. 6. In the low amplitude regime (green), a smooth line with a clear maximum and minimum can be found which resembles the behavior of the in-plane component of the particle stray field [17], similar to the situation shown in Fig. 4, $h = 100$ nm. With decreasing distance, the number of extrema increases strongly until the particle is placed directly on top of the sensor, where the extrema are superimposed by a characteristic with three distinct extrema (blue).

Within these regimes, different effects govern the sensor behavior:

1. *Linear answer regime* (green): The external magnetic influences on the sensor are small in comparison to the inter-particle dipolar coupling. The response of the device to the perturbation may be understood within the *linear answer theory*. As was already shown in Fig. 3(b), two- dimensional arrays only have a very low susceptibility for out-of-plane components. Therefore, the signal resembles the in-plane magnetic field contributions; perpendicular components are cancelled out.

2. *Boundary regime*: As indicated in Fig. 6(b), a strong increase of the signal can be found close to the boundaries of the systems. A probe particle position close in the center results in a much lower signal similar to the values obtained for the linear answer case. Here, boundary particles are affected.

3. *Domain regime*: The external magnetic field couples to the magnetic domain structure. The oscillating sign results from the antiparallel orientation along the domains. In particular, this can be seen in the particles assembly shown in Fig. 4. Lines of particles with antiparallel magnetization are passed when moving a particle along the *y*-axis.

4. *Direct answer regime*: The external source is very strong. The inter-particular coupling is overcome by the probe field and magnetic moments align with the external fields. Therefore, the response is proportional to the total magnetic field measured along the sensor plane and, consequently, resembles the magnetic field strength itself.

DOI: 10.5963/JBAP0202004

TABLE I ΔGMR-VALUES FOR DIFFERENT PROBE PARTICLE HEIGHTS AND MAGNETIZATIONS

	M_p in kA/m					
h in μm	1000	1200	1400	1600	1800	2000
0.02	0.0054	0.0062	0.0080	0.0080	0.0097	0.0098
0.03	0.0065	0.0084	0.0095	0.0099	0.0109	0.0125
0.04	0.0090	0.0103	0.0114	0.0127	0.0138	0.0144
0.05	0.0100	0.0125	0.0141	0.0148	0.0165	0.0185
0.06	0.0135	0.0148	0.0168	0.0187	0.0207	0.0227
0.07	0.0163	0.0190	0.0243	0.0307	0.0363	0.0381
0.08	0.0444	0.0500	0.0479	0.0522	0.0566	0.0577
0.09	0.1067	0.1058	0.1019	0.1071	0.1164	0.1247
0.1	0.1714	0.1939	0.2055	0.2013	0.2037	0.2035

TABLE II ΔGMR-VALUES FOR DIFFERENT PROBE PARTICLE HEIGHTS AND MAGNETIZATIONS

	M_p in kA/m					
h in μm	1000	1200	1400	1600	1800	2000
0.02	0,00084	0,001	0,0012	0,0014	0,0016	0,0017
0.03	0,0011	0,0014	0,0016	0,0018	0,0020	0,0022
0.04	0,0015	0,0018	0,0021	0,0024	0,0027	0,0029
0.05	0,0021	0,0025	0,0029	0,0032	0,0036	0,0039
0.06	0,0032	0,0036	0,0039	0,0044	0,0049	0,0054
0.07	0,0053	0,0058	0,0063	0,0067	0,0074	0,0081
0.08	0,0104	0,0115	0,0124	0,0136	0,0160	0,0185
0.09	0,0303	0,0432	0,0614	0,0719	0,0703	0,0865
0.1	0,0742	0,0863	0,0847	0,0898	0,0973	0,1036

Further, the measurement regime may be readily adjusted by the modification of the particle properties within the sensing layer as shown for the example of the particle magnetization, Fig. 7, left. If the magnetization is increased from 500 kA/m to 1000 kA/m, the coupling between contiguous particles is increased and the overall response is lowered. Numeric values can be found in Table 2. It needs to be pointed out that in both cases the active measuring mode seems to be directly related to the ΔGMR-value. However, this statement needs to be verified in future calculations.

It was already shown that a modification of the microstructural symmetry impacts the response properties. A comparison between ΔGMR-maps for cubic and hexagonal arrays emphasizes this observation. In particular, we find the hexagonally ordered assemblies to be significantly more sensitive than the cubic lattices. Such a behavior can be explained by the number of neighbors and the resulting stable magnetic structures. Similar to the situation of magnetocrystalline anisotropy where an increased number of easy directions (uniaxial → cubic → isotropic) results in a softer switching characteristic, the reduced number of neighbors for the cubic grid decreases the number of stable states. In particular, these structures form small vortices (compare Fig. 2). The magnetic response behavior of an elementary vortex structure is shown in Fig. 8. These substructures have a high stability, which results in a low susceptibility for small field values. High response may only be measured, once the vortex is broken.

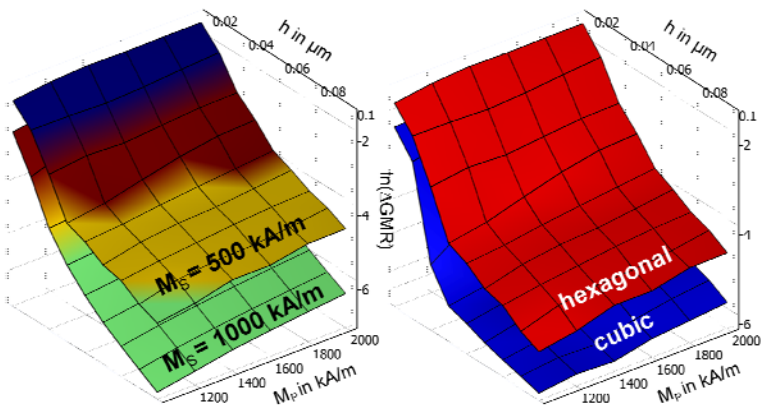

Fig. 7 (a) Intensity plots for different magnetization values of the layer components (upper: 500 kA/m, lower: 1000 kA/m)
A higher magnetic moment results in a strong coupling and, consequently, a shift towards lower response regimes.
(b) Response comparison between cubic (blue) and hexagonal (red) arrays

DOI: 10.5963/JBAP0202004

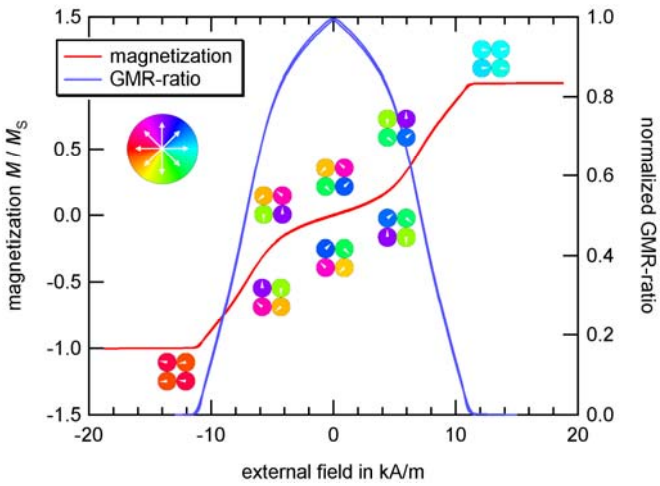

Fig. 8 Lowered response of cubic lattices due to high vortex stability
The magnetic response properties of an elementary vortex show a plateau of small susceptibility for small field values. An increase can be reported once the vortex structure is broken. The two sets of subplots in the figure highlight a reconfiguration of the vortex orientation after the structure was brought into magnetic saturation

V. EXTERNAL FIELD INFLUENCE

In order to study the basic properties of the granular sensor devices, additional external magnetic fields to bring the probe into saturation were neglected in the first step. In real systems, such fields will be important; otherwise, the superparamagnetic nature of the probe particle will not result in a magnetic field stable against thermal agitation.

Therefore, calculations under the assumption of an additional homogeneous magnetic field perpendicular to the particle plane were conducted. In dependency of the particle height, for probe magnetizations of 1000, 1400 and 1800 kA/m and external field values of 100, 200 and 300 kA/m, the results are shown in Fig. 9.

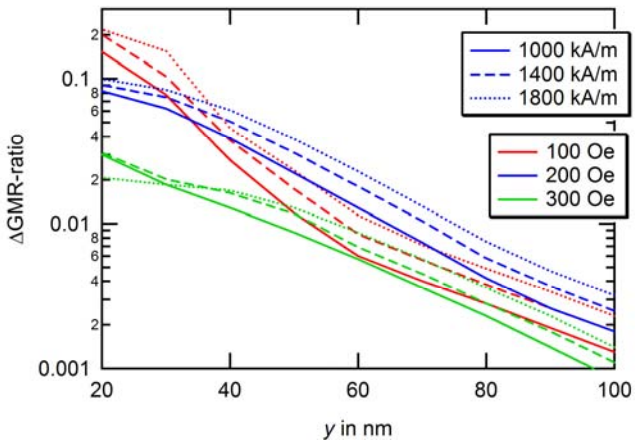

Fig. 9 ΔGMR-response for different probe particle heights,
probe particle magnetizations and external fields applied perpendicular to the particle plane

Especially, for the close distance observations, a low magnetic field seems to be favorable. The perturbation of a probe particle is not diminished by the external field and, hence, a transition to the direct measuring regime may occur. However, particles very close to the sensor only have very small in-plane components. If the particle is moved further away, the degree of in-plane components increases which may have a strong impact on the out-of-plane contributions induced by the external field which are not compatible with the high aspect ratio of the system. Within these regions, the external field has a destabilizing effect on the magnetic granular structure which results in a higher sensitivity as can be found in the comparison between the 100 and the 200 Oe field. Above a critical threshold, the dynamics are increasingly governed by the external field, which pins the moment directions, and a shift to lower measurement regimes is the result. In particular, a modification of the external field values offers an additional degree of freedom to tailor the granular sensor to a specific measurement task or to obtain more information in a static system exposed to a varying magnetic field.

VI. CONCLUSIONS AND OUTLOOK

We have presented numerical studies on arrays of dipolar coupled magnetic nanoparticles and analyzed their capability to

DOI: 10.5963/JBAP0202004

act as a magnetic field sensor. Apart from a wide range of modification possibilities to tailor the sensor response to a specific measurement task, we found four different operation modes of the proposed device. Each regime is governed by a specific system energy and is activated if the magnetic source impact along the surface surpasses a certain threshold. Again, the adjustment of either the nanocomponents or the geometrical nanostructure allows shifting the measurement regimes where direction depends on whether the inter-particular coupling is in- or decreased. Also, according to the numeric data, the measured GMR-amplitude is directly related to the apparent regime. More calculations need to be carried out in the future to verify this result.

In contrast to the continuous sensors, which, on the respective size scale, form the limit for exchange dominated systems, our analysis was carried out for the limit of pure dipolar coupling. The influence of a matrix material in between the particles results in an additional parallel coupling between adjacent particles and will be studied in future calculations. Also, the influence of thermal contributions needs to be studied. Due to the employed size-scale, the magnetic components are close to their superparamagnetic limit. Therefore, for the realization of the sensor, the question for suitable particle materials needs to be addressed.

ACKNOWLEDGMENT

The authors would like to thank the FOR 945 for financial support in the framework of the Project 3. Alexander Weddemann gratefully acknowledges financial funding from the Alexander von Humboldt foundation.

REFERENCES

[1] P. Grünberg et al., Phys. Rev. Lett. 57, p. 2442, 1986.

[2] M.N. Baibach et al., Phys. Rev. Lett. 61, p. 2472 (1988).

[3] J. Loureiro, R. Ferreira, S. Cardoso, P.P. Freitas, J. Germano, C. Fermon, G. Arrias, M. Pannetier Lecoeur, F. Rivadulla, J. Rivas. Appl. Phys. Lett. 95, p. 034104, 2009.

[4] S.X. Wang, G. Li, IEEE Trans. Magn. 44, pp. 1687-1702, 2008.

[5] A. Weddemann, C. Albon, A. Auge, F. Wittbracht, P. Hedwig, D. Akemeier, K. Rott, D. Meißner, P. Jutzi, A. Hütten. How to design magneto-based total analysis systems for biomedical applications. Biosens. Bioelec. 26, pp. 1152-1163, 2010.

[6] A. Weddemann, I. Ennen, A. Regtmeier, C. Albon, A. Wolff, K. Eckstädt, N. Mill, M.K.H. Peter, J. Mattay, C. Plattner, N. Sewald, A. Hütten, Beilstein J. Nanotech. 1, pp. 75 – 93, 2010.

[7] A. Hütten, D. Sudfeld, I. Ennen, G. Reiss, W. Hachmann, U. Heinzmann, K. Wojczykowski, P. Jutzi, W. Saikaly, G. Thomas, J. Biotech. 112, pp. 47-63, 2004.

[8] A. Moser, K. Takano, D. Margulies, M. Albrecht, Y. Sonobe, Y. Ikeda, S. Sun, E.E. Fullerton, J. Phys. D: Appl. Phys. 35, pp. R157-167, 2002.

[9] S. Sun, Adv. Mater. 18, pp. 393-403, 2006.

[10] A.E. Berkowitz, J.R. Mitchell, M.J. Carey, A.P. Young, S. Zhang, F.E. Spada, F.T. Parker, A. Hütten, G. Thomas, Phys. Rev. Lett. 68, pp. 3745 – 3748, 1992.

[11] J.Q. Xiao, J.S. Jiang, C.L. Chien, Phys. Rev. Lett. 68, pp. 3749 – 3752, 1992.

[12] L.D. Landau, E. Lifshitz, Phys. Z. Sowjetunion 8, pp. 153-169, 1935.

[13] A. Weddemann, A. Auge, D. Kappe, F. Wittbracht, A. Hütten, J. Magn. Magn. Mat. 322, pp. 643 – 646, 2010.

[14] V. Schaller, G. Wahnström, A. Sanz-Velasco, A´S. Gustafsson, E. Olsson, P. Enoksson, C. Johansson, Phys. Rev. B 80, 092406, 2009.

[15] N. J. Wiser, J. Magn. Magn. Mat. 159, pp. 119 – 124, 1996.

[16] A. Weddemann, A. Auge, C. Albon, F. Wittbracht, A. Hütten, New J. Phys. 11, p. 113027, 2009.

[17] C. Albon, A. Weddemann, A. Auge, K. Rott, A. Hütten, Appl. Phys. Lett. 95, p. 023101, 2009.

DOI: 10.5963/JBAP0202004